Published in final edited form as:
Nat Neurosci. 2010 April ; 13(4): 458–466. doi:10.1038/nn.2515.

Control of Sexual Differentiation and Behavior by the *doublesex* gene in *Drosophila melanogaster*

Elizabeth J. Rideout[1,3,4], **Anthony J. Dornan**[1,4], **Megan C. Neville**[1,2,4], **Suzanne Eadie**[1], and **Stephen F. Goodwin**[1,2]

[1]Faculty of Biomedical and Life Sciences, Molecular Genetics, University of Glasgow, Pontecorvo building, Glasgow G11 6NU, UK

[2]Department of Physiology, Anatomy and Genetics, University of Oxford, Sherrington Building, Parks Road, Oxford OX1 3PT, UK

Abstract

Doublesex proteins, part of the structurally and functionally conserved Dmrt gene family, play essential roles in sex determination throughout the animal kingdom. We targeted the insertion of GAL4 into the *doublesex* (*dsx*) locus of *Drosophila melanogaster*, allowing visualization and manipulation of *dsx* cells in various tissues. In the nervous system, significant differences between the sexes were detected in *dsx* neuronal numbers, axonal projections, and synaptic density. We show that *dsx* is required for the development of male-specific neurons that co-express *fruitless* (*fru*), a key regulator of male sexual behavior. We propose that both *dsx* and *fru* act together to form the neuronal framework necessary for male sexual behavior. Significantly, we show that disrupting *dsx* neuronal function has profound effects on male sexual behavior. Furthermore, we demonstrate a role for *dsx* neurons in pre- through to post-copulatory female reproductive behaviors.

Significant insights into the genetic and developmental logic supporting sex-specific behaviors have come from the genetically and behaviorally tractable model organism, *Drosophila melanogaster1*. In *Drosophila*, genes of the sex-determination hierarchy orchestrate the development and differentiation of sex-specific tissues, establishing sex-specific physiology and neural circuitry2. Female-specific expression of Transformer (Tra), with the non-sex-specific Transformer-2, introduces a sex-specific splice in two pivotal downstream transcription factors, *doublesex* (*dsx*) and *fruitless* (*fru*). In females, *dsx* transcripts are spliced to give rise to a female-specific isoform: Dsx^F. In contrast, sex-specific splicing introduces a stop codon into female-specific *fru* mRNAs, which are then not translated. In males, in the absence of Tra, *dsx* and *fru* transcripts undergo default splicing, generating the male-specific isoforms: Dsx^M and Fru^M. Together, these key transcriptional regulators establish most aspects of ‘maleness’ and ‘femaleness’.

Dsx proteins are part of the Dmrt (*doublesex* and *mab-3*-related transcription factor) family, a structurally and functionally conserved group of zinc-finger transcription factors with important roles in sex determination throughout the animal kingdom3. In *Drosophila dsx*

Correspondence should be addressed to S.F.G. (stephen.goodwin@dpag.ox.ac.uk). .
[3]Present Address: Department of Biochemistry and Molecular Biology, University of Calgary, HRIC 2A33, 3330 Hospital Drive, Calgary, AB, T2N 4N1.
[4]These authors contributed equally to this work.
Authorship Contribution
E.J.R., A.J.D, M.C.N., and S.F.G. designed experiments and wrote the paper. E.J.R., A.J.D, and M.C.N. all contributed equally to performing the experiments. S.E. provided technical assistance.

Europe PMC Funders Author Manuscripts

directs most aspects of somatic sexual differentiation outside the central nervous system (CNS) in both sexes. Many of these differences are implicated in the performance or success of male sexual and reproductive behaviors4-9.

Many recent studies have focused on the control of sexual behavior in males by *fru*10-12. Fru^M proteins are expressed from metamorphosis in the male CNS13. In the absence of Fru^M proteins, males perform little to no courtship towards females, fail to produce the pulse song component of generate aberrant courtship song, never attempt copulation, and exhibit increased inter-male courtship2. Females expressing Fru^M display many male-specific courtship behaviors; however, they court less than wild-type males, generate aberrant song and never attempt copulation11, 14. Thus Fru^M expression is not sufficient to specify normal male courtship behavior, suggesting other genes are required for a complete male courtship repertoire.

One obvious candidate is *dsx*. Males lacking *dsx* court at diminished levels and generate aberrant fail to generate the sine song component of courtship song15. Dsx is found in the CNS14, 16, 17, and Dsx^M and Fru^M proteins are co-expressed in several regions important in establishing male sexual behavior14, 18. Recent studies suggest that *dsx* and *fru* co-operate to dictate development of specific neural substrates underlying male sexual behavior14, 18-20, thus both genes, are necessary in the specification of neural systems that generate male patterns of behavior21. However, little is known about the neuroanatomical expression of *dsx* in the CNS and how this influences male and female sexual behavior.

To explore the anatomy and function of *dsx*-expressing neurons in both sexes, we targeted the insertion of the yeast transcription factor GAL4 to the *dsx* locus. Clear differences in neuronal numbers and axonal projections were detected in male and female CNSs. These differences are behaviorally relevant, since disrupting *dsx* neuronal function leads to highly aberrant behaviors in both sexes, suggesting these neurons instruct sex-specific neural programs. We propose that *dsx* co-ordinates the development of external sexual morphology and physiology with the development of sex-specific neurons that contribute to the circuitry required for male and female sexual behaviors.

Results

Targeting GAL4 to the *doublesex* locus

To allow detailed anatomical and functional analyses of *dsx*-expressing cells we used ends-in homologous recombination to insert the GAL4 coding sequence into the first, non-sex-specific, coding exon of *dsx*, creating a tandem duplication at the locus (Fig.1a and Supplementary Fig. 1 online). The resulting allele, dsx^{GAL4}, produces wild-type *dsx* transcripts, as well as GAL4-containing transcripts in both sexes (Fig. 1b and Supplementary Fig. 1). When homozygous, or examined *in trans* to a deficiency of *dsx* ($Df(3R)dsx^{15}$), external sexual morphology (data not shown) and fertility of dsx^{GAL4} flies were unaffected ($p>0.05$, $n>45$). We conclude the dsx^{GAL4} allele exhibits no overt disruption of gene function.

To determine whether dsx^{GAL4} reiterates endogenous *dsx* expression, we used dsx^{GAL4} to drive expression of a nuclear reporter demonstrating co-localization with all previously described Dsx-expressing neuronal clusters16 (Fig. 1c,d). Thus dsx^{GAL4} is a sensitive, specific marker for Dsx-expressing cells.

dsx^{GAL4} cells dictate sexual differentiation

dsx is required to establish sexually dimorphic morphology and characteristics in male and female flies22, but it is unclear where Dsx is expressed, and whether *dsx* cells dictate all

aspects of external sexual morphology. We determined the temporal and spatial distribution of *dsx*^{GAL4} cells (Supplementary Fig. 2 online). *dsx*^{GAL4} expression was observed in a number of tissues with sexually dimorphic features or physiology, such as the foreleg, cuticle, oenocytes, fat body, and reproductive organs. *dsx*^{GAL4}-expression however is not ubiquitous, suggesting that sex determination need not occur in every cell. Are these *dsx*^{GAL4} cells capable of controlling sexual differentiation?

dsx's ability to determine secondary sexual characteristics has been established through mutant analyses, or ubiquitous over-expression of Dsx isoforms22. To determine if *dsx*^{GAL4}-expressing cells are capable of directing a sex-specific program of development, we restrictively manipulated the sex of *dsx*^{GAL4}-expressing cells, assaying the consequences of expressing either Dsx^{M} or Dsx^{F} to external sexual morphology. Dsx^{F} over-expression resulted in single-X males with female-like abdominal pigmentation, genitalia, and no sex combs. (Fig. 1i); thus Dsx^{F} is sufficient to direct a female-specific program of development even when competing with endogenous Dsx^{M} production. Dsx^{M} over-expression resulted in masculinized XX females that displayed male-like abdominal pigmentation and sex combs; however the genitalia, while masculinized, were rotated and often malformed (Fig. 1j), possibly due to an inability to overcome the effects of endogenous Dsx^{F}.

XX flies homozygous for loss-of-function *tra* or *tra-2* mutations develop as pseudo-males; they are essentially indistinguishable from males in morphology and behavior, though sterile23-25 (Fig. 1h). Using RNA interference we specifically knocked-down endogenous Tra and Tra-2 in *dsx*^{GAL4} cells. Strikingly, XX flies developed as close phenocopies (Fig. 1k,l) of *tra* and *tra-2* loss-of-function variants; they exhibited male-like abdominal pigmentation, genitalia, and sex combs. *dsx*^{GAL4} cells are therefore capable of directing sex-specific morphological development.

dsx-specified sexually dimorphic neural circuitry

While *dsx*'s specification of external sexual morphology influences sexual behavior5, 26, the anatomical foci central to determination of sex-specific behaviors lie in the CNS2. Therefore, we used *dsx*^{GAL4} to describe dimorphic *dsx* expression in the developing CNS (Fig. 2; Supplementary Fig. 3, and Supplementary Table 1 online).

In addition to previously described *dsx*-pC1, -pC2 and -aDN neuronal clusters in the adult posterior brain16, we identified a novel *dsx*-expressing cluster, designated *dsx*-pC3 (Fig. 2a,d,m,n; Supplementary Table 1). The pC1, pC2 and pC3 clusters have higher numbers of neurons in males (Fig. 2a vs. Fig. 2d; Supplementary Table 1). These neurons lie in the dorsal inferomedial, inferolateral and superomedial protocerebrum (respectively) surrounding the mushroom body calyces, sites implicated in sex-specific behaviors in both sexes2 (Fig. 2m,n; Supplementary Fig. 4 online). In the suboesophageal ganglion (SOG), two male-specific neurons, *dsx*-SN, are present (Fig. 2a-c).

Despite the striking dimorphism in neuronal numbers in the brain, the topology of *dsx*-neuronal projections was remarkably similar between male and female brains. The most overt difference is the dramatic increase in density of synapses and projections in males compared to females as determined by visualization of pre-synaptic and membrane markers in *dsx*^{GAL4} neurons (Fig. 2b,c,m vs. Fig. 2e,f,n; Supplementary video 1 online).

In both sexes these bilateral dorsal clusters are extensively interconnected (ipsilaterally, with projections extending throughout the medial and lateral protocerebrum; and contralaterally, via an extensive commissural bridge in the superior protocerebrum, to clusters in the opposing hemisegment)20. These connections also extend to the SOG, the point of

termination for projections originating directly and indirectly from tarsal gustatory neurons, implicated in mate choice via processing of non-volatile pheromonal cues27.

In the ventral nerve cord (VNC), adult males exhibit expression in the described male-specific *dsx*-TN1 neuronal clusters and -TN2 cells (Fig. 2g)16. The TN1 neuronal clusters appear to communicate directly with each other, with locally associated TN2 cells, and with regions in the brain responsible for higher order processing of sensory cues via projections through the cervical connective (**Fig.** 2i,j and 3f; Supplementary video 2 online). It is noteworthy that the ventral Msg, a focus for male-specific unilateral wing extension and courtship song, is innervated by male-specific TN1 and TN2 neurons14, 28, 29. Thus dsx^{GAL4} reveals significant dimorphism between males and females in neuronal number, axonal projections and synaptic density in behaviorally relevant regions of the brain.

Extensive innervation in the ventral prothoracic ganglia (Prg) occurs in both sexes. In males these project ipsilaterally, connecting with TN2 cells, as well as contralaterally to form a distinct commissural bridge (**Fig.** 2i,j and 3f). Females exhibit only ipsilateral projections (**Fig.** 2k,l and 3h). Previous studies demonstrated gustatory receptors in the foreleg exhibit a similar sexual dimorphism30. The male foreleg exhibited a significant difference in dsx^{GAL4} cell numbers, in both metatarsus and tarsi 2-5, compared to females (Fig. 3a vs Fig. 3d). Some of these cells are neuronal, as fewer cells were observed when expression of GAL80, a GAL4 repressor, was targeted to postmitotic neurons using the *elav* promoter (Fig. 3e). More cells were repressed in males than females, indicating there are more neurons in the male foreleg.

As axons degenerate when severed31, we amputated forelegs of dsx^{GAL4} flies expressing membrane-bound GFP. Amputating male forelegs below the sex comb, or an equivalent point in females, showed no overt degeneration in projections (data not shown). With amputations performed above the sex comb, or equivalent point in females, no foreleg projections were observed (Fig. 3g,i). Since only gustatory neurons cross the midline in male VNCs30, at least some of the male dsx^{GAL4}-projections are from gustatory neurons involved in non-volatile taste sensation.

The abdominal ganglion (Abg), the anatomical foci for copulatory behaviors in males and females1, is the sole region of the VNC where dsx^{GAL4} expression occurs in both sexes, with adult females exhibiting expression in a larger number of cells (Fig. 2g,h; Supplementary Table 1). Neurons from this region send projections through the abdominal nerve trunk to ramify the internal genitalia in both sexes (data not shown). In males four bilateral pairs of axonal fascicles run through the cervical connection, connecting the brain and VNC (Fig. 2i). In females there are five bilateral pairs of axonal fascicles, perhaps reflecting the increased neuronal expression apparent in the Abg (**Fig.** 2k and 3h).

In summary, we found dsx^{GAL4} expression in ~900 neurons (9 groups) in males, and ~700 neurons (5 groups) in females in the adult CNS (Supplementary Table 1). In the development of these neurons, we highlight 48 hr pupae as a critical point of divergence between the sexes. At this stage SN and TN2 cells arise in both sexes (later disappearing in females), TN1 neuronal clusters appear in males (but never females), and until this stage, the number of dsx^{GAL4}-Abg neurons is consistently higher in males (Supplementary Fig. 3 and Supplementary Table 1).

Our examination of dsx^{GAL4} neurons clearly demonstrates significant differences in cell numbers, projections and synaptic density in regions of the CNS associated with sex-specific behavior. We speculate that assembly of these neural networks, and their sex-specific differences, are responsible for the differences in male and female behavioral programs.

dsx and *fru* specify sexual dimorphisms in the CNS

Dsx^{M} and Fru^{M} are co-expressed in a restricted number of regions within the male CNS14, 18, 20. We found *dsx*^{GAL4}-expressing neurons reiterated this co-localization with Fru^{M} (Fig. 4). Both Dsx^{M} and Fru^{M} expression are required for the complete development of a number of specific neuronal populations within the male CNS14, 18, 20. Therefore, to examine the contributions of *fru* and *dsx* to the specification of *dsx*^{GAL4}-expressing neurons, we counted the number of *dsx*^{GAL4} neurons in *fru* and *dsx* mutant backgrounds (Fig. 5 and Table 1).

In Fru^{M}-null males (expressing Dsx^{M} but lacking Fru^{M}), *dsx*-pC1, -pC2 and -pC3 neuronal numbers were significantly reduced compared with wild-type (Fig. 5c,d). A significant reduction in the density of axons was observed in the cervical connection and in the contralateral connections in the Prg (Fig. 5f). No reduction in *dsx*-SN, -TN1, or -TN2 clusters was observed (Fig. 5e); however we have previously shown a Fru^{M}-dependent reduction in *dsx* cells in the Abg18. Fru^{M} is therefore required for the full complement of *dsx*^{GAL4} neurons. To test whether Fru^{M} is sufficient to specify *dsx*^{GAL4} neurons, we counted *dsx*^{GAL4} neurons in females expressing Fru^{M}, and found the number of *dsx*^{GAL4} neurons was not significantly different from wild-type females (Fig. 5g-j). This demonstrates that Fru^{M} expression is not sufficient to specify complete development of male-specific circuitry, as previous studies suggested11.

To determine if *dsx* is sufficient to specify this neural circuitry, we counted *dsx*^{GAL4} neurons in females expressing both Dsx^{F} and Dsx^{M}. Neuronal numbers were significantly increased in -pC1, -pC2, and -SN (but not -pC3) in the brain, and all VNC clusters compared to wild-type females with a concomitant increase in projections and formation of contralateral connections (Fig. 5k-n; Table 1). However, the number of *dsx*-pC1 and -pC2 neurons was still significantly lower than wild-type males (Table 1). Since Dsx^{F} precipitates Programmed Cell Death (PCD) in ~20 cells of the *fru*-P1 neuronal cluster20; and this cluster is a sub-population of *dsx*-pC1, a reduction in overall cell number in Dsx^{M}-expressing females is expected. Similar cell-death processes may occur in the pC2 and pC3 clusters.

Sex-specific PCD is one mechanism for creating sexual dimorphism in the brain12, 20. Thus we investigated its role in sculpting the *dsx* circuitry by expressing the cell-death inhibitor *p35* in *dsx*^{GAL4} cells32; and counting the number of neurons in adult females. *dsx*-SN and -TN2 cells, present in both sexes in 48hr pupa but specific to males in the adult (Supplementary Table 1), were protected from PCD, as their numbers were not significantly different from wild-type males (Fig. 5o,p; Table 1). Additional neurons were observed in -pC2 and -pC3 clusters as well as cells of the TN1 cluster (3± 0.4, n=14; Fig. 5o-s), which are never observed in females. Intriguingly when TN1 and TN2 neurons are present in females they display contralateral projections ordinarily seen only in wild-type males (Fig. 5q).

Taken together, these results demonstrate that Dsx^{M} and Dsx^{F} are the primary regulators of dimorphisms in *dsx*^{GAL4} neurons, though Fru^{M} function is required to obtain a full complement of male-specific *dsx*^{GAL4} neurons, and that sex-specific PCD is one mechanism used to assemble this dimorphic circuitry. Importantly, we show that small changes in neuronal populations can significantly alter the organization and connectivity of the neural network that presumably forms the anatomical basis for sex-specific behaviors.

dsx^{GAL4} neurons are required for male sexual behavior

dsx mutant males display aberrant courtship but the neural etiology for this abnormality is unknown2. Having shown that *dsx* is required in the construction of sex-specific neural substrates; we asked whether *dsx*-expressing neurons play an active role in courtship behavior. We quantified fertility and courtship behavior in males expressing *UAS*-tetanus

neurotoxin light chain (TNT), which targets neuronal synaptobrevin33, in dsx^{GAL4} neurons. After one week in the presence of several virgin females, these males were completely infertile (n=60) (Fig. 6a). We next determined whether the infertility was a consequence of defects in courtship and/or mating. The time taken for $UAS\text{-}TNT_G;dsx^{GAL4}$ males to initiate courtship was significantly increased (Fig. 6b), and once courtship was initiated, the amount of courtship performed was severely reduced and consisted entirely of intermittent following and orientation with no attempted copulation (Fig. 6c). These males did not extend their wings and there was a complete absence of sine- and pulse-courtship song (Fig. 6e).

During an extended 4hr observation period, ~95% of control flies successfully copulated, but no $UAS\text{-}TNT_G;dsx^{GAL4}$ males copulated (Fig. 6d). Courtship defects in $UAS\text{-}TNT_G;dsx^{GAL4}$ males cannot be explained by more general defects in morphology or sensorimotor function because $UAS\text{-}TNT_G;dsx^{GAL4}$ males do not exhibit gross anatomical abnormalities in their genitalia or reproductive systems, including neuronal innervation (data not shown), and performed at least as well as wild-type and control males in assays for locomotion, flight, olfaction, and taste (Supplementary Fig. 5 online).

Thus inhibition of dsx^{GAL4} neuronal function in males disrupts the early steps of courtship (orientation, following) and the complete absence of the later steps (wing extension, courtship song and attempted copulation) suggesting that *dsx* neurons directly and specifically contribute to male courtship behaviors.

Since dsx^{GAL4} is expressed in a variety of tissues outside the nervous system (Supplementary Fig. 2), we tested whether aberrant courtship behavior in $UAS\text{-}TNT_G;dsx^{GAL4}$ males results from disruption of neural function. We used *elav-GAL80* to inhibit GAL4-driven expression of TNT specifically in neurons. *elav-GAL80* specifically and comprehensively inhibits neural expression of GFP in dsx^{GAL4}; *UAS-nGFP* flies, validating the efficacy of this tool (Supplementary Fig. 3k). Removing TNT expression specifically from neurons reversed the observed courtship defect. Males expressing $UAS\text{-}TNT_G$; $elav\text{-}GAL80,dsx^{GAL4}$ showed greatly improved levels of fertility (Fig. 6a), courtship initiation (Fig. 6b), and a significant recovery in their CI's (with consequent restoration of courtship modalities such as licking, tapping, and wing extension) when compared with $UAS\text{-}TNT_G;dsx^{GAL4}$ males (Fig. 6c). The percentage of males copulating within a 4-h observation period was also significantly improved (Fig. 6d), as was the ability to produce both sine- and pulse-song bouts (Fig. 6e). These results demonstrate the aberrant courtship phenotypes of $UAS\text{-}TNT_G;dsx^{GAL4}$ males were largely a consequence of disrupting dsx^{GAL4} neuronal function. That not all behaviors were restored to control levels likely reflects the inability of GAL80 to fully repress GAL4 function. Collectively, these results demonstrate that dsx^{GAL4} neurons are required for male courtship behavior.

dsx^{GAL4} neurons are critical for female sexual behavior

The neurobiological basis of female sexual behavior is poorly defined, though it was suggested that *dsx*'s influence on the sex of the CNS might be critical to female behavior8. We investigated the effects of disrupting dsx^{GAL4} neuronal function on female behavior through expression of TNT (Fig. 7). To confirm the neuronal contribution of dsx^{GAL4} cells to female sexual behavior, we also used *elav-GAL80* to restrict expression of TNT to non-neuronal tissues.

$UAS\text{-}TNT_G;dsx^{GAL4}$ females were completely infertile (Fig. 7a), and laid no eggs over five consecutive days post-mating (Fig. 7b). Over time the abdomens of these females became distended, with extruded ovipositors (Supplemental Fig. 6a) and mature eggs atrophying in their oviducts (Supplemental Fig. 6b).

We next observed the courtship behavior of *UAS-TNT*$_G$; *dsx*^{GAL4} virgin females paired with individual wild-type males. Initially the percentage of females copulating in a 1-h period was investigated (Fig. 7c). Virgin *TNT*$_G$; *dsx*^{GAL4} females were less receptive than control females within the first 10 minutes (<30% vs. >96%, respectively) but by 40 minutes the percentage of *TNT*$_G$; *dsx*^{GAL4} females that had copulated was near control levels (>93% and 100%, respectively).

We then investigated *UAS-TNT*$_G$;*dsx*^{GAL4} females' behavior during, and several hours after, copulation. During copulation, these females actively rebuffed males, exhibited sustained wing flicks, kicking, and failed to remain stationary (Supplementary Video 3 online). Although males often manage to grasp hold of a female, they never manage to spread the female's wings during copulation. The result of this aberrant copulation with *UAS-TNT*$_G$;*dsx*^{GAL4} females was a dramatic increase in locomotion of copulating pairs (Fig. 7d; Supplementary Video 3) compared to controls. Indeed we found a significant decrease in the length of copulation with *UAS-TNT*$_G$;*dsx*^{GAL4} females compared with controls, presumably a consequence of the vigorous rejection displayed by these females (Fig. 7e). Intriguingly, during a 4-h observation period, approximately 30% of *UAS-TNT*$_G$;*dsx*^{GAL4} females were observed to re-mate with the same male, some as many as four times (Fig. 7f), though they continued to exhibit vigorous rejection behaviors throughout. Control females never re-mated during the observation period.

The observed infertility of *UAS-TNT*$_G$;*dsx*^{GAL4} females was not due to a lack of sperm transfer during the shorter copulation time, as the reproductive tracts of females who copulated with males with the sperm-enriched mitochondrial marker Don Juan-GFP, were positive for GFP (Supplementary Fig. 6h online)34. We also confirmed transfer of seminal fluids, required for post-mating rejection responses, using a transgene encoding the accessory gland protein Sex-peptide fused to GFP (Supplementary Fig. 6f)35. That no 'live births' were observed suggests this infertility is due to an inability to deposit eggs into the uterus, preventing sperm, stored in the seminal receptacle and spermathecae, from fertilizing the mature oocyte. *UAS-TNT*$_G$;*dsx*^{GAL4} females exhibited no gross anatomical abnormalities in the genitalia or reproductive system, including their neuronal innervation (data not shown); and they performed at least as well as wild-type and control females in assays for locomotion, flight, olfaction, and taste (Supplementary Fig.5).

To interrogate the unusual re-mating phenotype, we compared post-mating responses in mated *UAS-TNT*$_G$;*dsx*^{GAL4} females against mated control females, and retested for receptivity 24-h later with a second naïve male. During a 1-h observation period 69% of mated *UAS-TNT*$_G$;*dsx*^{GAL4} females re-mated (n=13), while no mated control females re-mated (n=14). In addition, male courtship behaviors were not suppressed by mated *UAS-TNT*$_G$;*dsx*^{GAL4} females, as wild-type *Drosophila* females ordinarily do post-mating2; rather they continued to elicit vigorous courtship (CI= 82.4% ± 4.4) compared with mated control females (CI=28.4% ± 6).

To confirm the infertility and courtship defects observed were a consequence of disrupting *dsx*^{GAL4} neurons, we used *elav-GAL80* to inhibit GAL4-driven neuronal expression of TNT. Fertility and egg laying in *UAS-TNT*$_G$;*elav-GAL80,dsx*^{GAL4} females was not appreciably different from controls (Fig. 7a and 7b). Similarly, locomotion during copulation, copulation duration, and re-mating after copulation, were restored to wild-type levels (Fig. 7d-f). This suggests that the abnormal behaviors exhibited by *UAS-TNT*$_G$;*dsx*^{GAL4} females were a result of disrupting *dsx*^{GAL4} neurons. These results demonstrate that *dsx*^{GAL4} neurons play a critical role in female courtship and reproductive behaviors. In particular, *dsx*^{GAL4} neurons appear to be important for receptivity to copulation and mating-induced behavioral changes.

Discussion

Using the novel *dsx*^{GAL4} allele we have been able to comprehensively describe *dsx* expression in neuronal and non-neuronal tissues throughout development. By manipulating the sex of *dsx*^{GAL4}-expressing cells we demonstrated their ability to direct a sex-specific program of morphological development. We also identified profound dimorphisms in neural circuitry in males and females; from differences in cell numbers in homologous clusters; to sex-specific neuronal development; to density, organization and connectivity of axonal projections. Specific inhibition of the function of these neurons in the males and females resulted in disruption of distinct sex-specific behavioral outputs, suggesting that differences in neuroanatomy instruct sex-specific behaviors.

In males significant overlap between *fru*- and *dsx*-expressing neurons occurs, allowing functional roles for certain *dsx* neurons to be inferred from their intersection with *fru* neurons with defined roles in male sexual behavior14, 20, 36. In males *dsx*-pC1 colocalizes with the medial *fru*-P cluster (Fig. 4a), a focus for licking and copulatory behaviors37-39. *dsx*-pC1 intersects with a subset of *fru*-P1 neurons, with a demonstrated role in courtship initiation and whose sexual differentiation and axonal morphology is dependent upon both *fru* and *dsx20*. *dsx*-pC2 colocalizes with the lateral *fru*-P cluster20 (specifically P2-P4; Fig. 4a), and *dsx*-pC3 colocalizes with the *fru*-pSP2 cluster (Fig. 4a), both regions of the brain associated with initiation, following, tapping and wing extension37-39. Projections to the ventral SOG show intense synapses positionally associated with the *fru*-mCAL, a region implicated in control of sequential courtship steps13, 40 (Fig. 2c). This coexpression of Fru^{M} and Dsx^{M} implies cooperation in shaping a shared male neural circuitry, an observation supported by the demonstrated reduction in *dsx*^{GAL4} neurons in pC1, pC2 and pC3 clusters in Fru^{M}-null males, analogous to the cooperation demonstrated in the Abg, or Msg14, 18. Early studies identified the ventral Msg as a neural focus for wing extension and song production28. More recently successful song production was correlated with the presence of a male-specific neuronal population in the Msg, and the existence of a localised song pattern generator in the Msg14, 29. Again significant overlap between *fru*- and *dsx*-expressing neurons is apparent in the VNC (Fig. 4b). *dsx* significantly increases neural complexity in this region by specifying the appearance of male-specific neurons and dimorphic projection patterns. Further complexity arises from the *dsx*-dependent dimorphism in axonal projection paths in the Prg (ispilateral in females versus contralateral in males), which appear to arise as a consequence of inputs from male-specific gustatory receptor neurons in the foreleg30. These receptors have a demonstrated role in non-volatile pheromonal gustation associated with male-specific tapping behaviors in courtship27.

That these *dsx*^{GAL4} neurons direct male-specific behaviors is supported by our finding that male courtship is impaired when their neural function is specifically disrupted. Therefore while *fru* is necessary in specifying male sexual behaviors, it is not sufficient; rather *dsx* is also required for complete specification of male courtship behaviors.

Male courtship behaviors, being robust and quantifiable, have long been the focus of behavioral genetics; however, males are not the only participants in copulatory bouts. Females appear superficially passive but exhibit subtle behaviors, consisting mostly of ‘rejection’ behaviors such as wing flicking or kicking2. Little is known about the effects these ‘rejection’ responses have on courting males, and what stimuli trigger these behaviors. From the female’s perspective however she must be able to assess a courting male to make an assured judgment of species type before she will sanction mating. Increased receptivity is indicated when a female slows down and ceases ‘rejection’ behaviors. It is worth noting that some species of Drosophilids actually exhibit an acceptance posture. While no clear acceptance posture has been demonstrated in *melanogaster* our findings suggest female

cooperation does occur to facilitate copulation. A neural focus for receptivity has been identified in the dorsal female brain2; it seems likely that dsx^{GAL4} neurons in this region contribute to female mating decisions, just as homologous neurons in males are involved in male decisions20, 41. This is supported by our findings that disrupting synaptic activity of dsx^{GAL4} neurons in females impairs distinct female courtship behaviors. These females are seemingly incapable of sampling the male's display, and so incapable of providing any acceptance response. When copulation occurs, lack of female cooperation is evidenced by continuous movement and rejection behaviors. While sperm and seminal fluids are successfully transferred to $UAS\text{-}TNT_G;dsx^{GAL4}$ females, they lay no eggs, re-mate, and remain incapable of actively rejecting or suppressing further courtship. This indicates that disrupting *dsx* neuronal function in females also suppresses post-mating behaviors, and implies that some of these neurons relay information from fru^+-sensory neurons in the female reproductive tract in response to Sex-peptide42, 43.

We have demonstrated that dsx^{GAL4} cells not only can reprise the functional roles of endogenous *dsx* in establishing external sexual morphology but also establishes a dimorphic neuroanatomy capable of directing distinct sex-specific behavioral outputs. In addition, dsx^{GAL4} expression occurs in sexually physiologically relevant non-neuronal adult tissues such as the fat body and oenocytes, whose correct sexual identity is critical to normal sex-specific behaviors8, 9, 44. Our findings indicate that adult sex-specific behaviors may arise as a consequence of changes to distinct cell groups during development, creating dimorphic neural circuitry in equivalent regions of the male and female brain. Our results demonstrate a fundamental requirement for *dsx* in the sexual development of both neuronal (sex-specific circuitry) and non-neuronal tissues (sex-specific physiology). Future studies will be aimed at identifying how *dsx* effects these dimorphic changes, refining our understanding of how individual *dsx* neurons instruct sex-specific neural programs, and at identifying the relative contributions of both "mind" (fly brain) and body to these behaviors.

Supplementary Material

Refer to Web version on PubMed Central for supplementary material.

Acknowledgments

We thank Toshiro Aigaki, Paul Breslin, Barry Dickson, Jean-Francois Ferveur, Frank Hirth, Gyunghee Lee, Renate Renkawitz-Pohl, Yikang Rong and Sean Sweeney for providing valuable reagents and protocols, and Jean-Christophe Billeter, Jeff Hall, Joel Levine, Brian Oliver and Scott Waddell for comments on the manuscript. We also thank members of the Goodwin lab for helpful discussions. This work was supported by grants from the Wellcome Trust.

Appendix

Methods

Targeted Insertion of GAL4 into the *dsx* Locus

GAL4 was targeted to the *dsx* locus by ends-in homologous recombination as previously described45, and as illustrated in Supplemental Fig. 1a. Three fragments with homology to the *dsx* genomic region were cloned sequentially into the targeting vector pED22 (generously provided by B. Dickson) using the following primers (5′ to 3′): Fragment I ggatcccactaaacgagaatcaaaaac and tctagagagaaagaccctgctggctatcag, Fragment II cctaggcttaaagtggctcttcggagg and ggatccgattccagcttctgatatccta, Fragment III gcggccgcacaaaactttcacccaactcaata and gcggccgcttgtctgccaggggtttttcag. The resulting construct was injected into a w^{1118} strain. One of the ensuing second chromosome transformant lines, was crossed (2000 virgin females) to males of the genotype *y,w/Y,hs-*

hid; Sco,hs-I-SceI,hs-FLP/CyO; first instar larvae were heat shocked for 1.5 hrs at 38°C on the 3rd day following the cross and again on the following day for 1hr. The following fly stocks were used to identify and balance all third chromosomal *white*$^{+}$ recombinants: *y,w; ey-FLP, y,w,ey-FLP; Pin/CyO, y,w,ey-FLP;;Ly/TM3,Sb* (provided by B. Dickson). Approximately 150,000 flies were screened, and 11 independent targeted recombination events were recovered. PCR, sequencing, and Southern blot analysis were used to confirm the predicted recombination event in multiple lines (data not shown). Two lines were selected for further analysis using multiple *UAS*-reporter transgenes and both exhibited equitable patterns of expression (data not shown); a single line was then chosen for all further studies. Using a *hs-CreI* expressing line (*w*^{1118}; *P{hs-ICreI.R}1A,Sb*^{1}*/TM6*), we attempted to reduce the duplication at the *dsx* locus, however after screening >50,000 flies, we were unable to recover a resolved line; this is likely due to a polymorphism subsequently discovered in the *I-CreI* site in the targeting vector pED22 (J. Walker, unpublished data).

D. melanogaster Strains and Crosses

Fly strains were raised as previously described46, unless stated otherwise. Wild-type flies obtained from *Canton-S* strain. Generation of *dsx*^{GAL4} allele strain as per Supplementary Fig.1. *dsx*^{GAL4} lines and all transgenes are in a *w*$^{+}$ background for behavioral studies. *dsx*$^{\mathrm{Dom}}$ allele was *dsx*^{Swe}. *fru*$^{\mathrm{M}}$ and *fru*$^{\mathrm{F}}$ alleles were examined *in trans* to *Df(3R)fru*$^{4\text{-}40}$. Transformation experiments employed a *Dp(1:Y)B*^{S}; *dsx*^{GAL4} */TM3, Sb* stock; haplo-X vs. diplo-X progeny identified by *Bar*-marked *Y* chromosome. RNAi crosses were performed at 29°C and used *UAS-tra*^{IR} No.2560 and *UAS-tra-2*^{IR} No.8868 (purchased from the Vienna Drosophila RNAi Center). Other transgenic lines used: *UAS-pStingerII, UAS-mCD8::GFP, UAS-RedStinger/CyO, UAS-LacZ.NZ* J312 (Bloomington Drosophila Stock Center), *UAS-synaptotagmin–HA, UAS-dsx*^{M}*,UAS-dsx*^{F}*, elav-GAL80* (provided by Sean Sweeney, University of York, UK), *y,w FRT19a; UAS-nlacZ,UAS-mCD8::GFP, UAS-p35; MKRS*/+ (provided by Frank Hirth, King's College London, UK), *w**; *P{dj-GFP}, w**; *P{SP-GFP}* and *UAS-TNT*$_{G}$.

Immunohistochemistry

All samples dissected and treated as previously described13, 46. See Supplementary Table 2 online for antibody details. Images and cell counts acquired as previously described13, 46. Epifluorescence microscopy performed on a Zeiss SteREO Lumar V.12 Stereomicroscope, captured via a Zeiss Axiocam. Axonal degeneration experiments involved severing newly eclosed flies' legs, CNSs dissected seven days later.

Behavioral Assays

For *UAS-TNT*$_{G}$ experiments flies were raised at 21°C in a 12hr:12hr light:dark cycle. Individual virgin adults were collected and aged for 5-7 days post-eclosion at 25°C and assays carried out at 25°C. Locomotion, male courtship index (CI) and song were recorded in round courtship chambers (1 cm diameter × 4 mm height), courtship latency measured in larger round chambers (2 cm diameter × 4 mm height). Fertility, latency, CI and duration were measured as previously described18. Sperm/Sex-peptide transfer, song analyses and locomotion during copulation were measured as previously described8, 14, 35.

Statistics

Behavioral means compared using Tukey-Kramer HSD statistical test where indicated. For Fisher's exact test, 2-tail p-values were compared to wild-type. Egg laying data subjected to Dunnett's test with wild-type as the set control. Cell counts were subjected to Student's t-test. Statistical tests performed with JMP v6.0 software (SAS Institute).

References

1. Dickson BJ. Wired for sex: the neurobiology of Drosophila mating decisions. Science. 2008; 322:904–909. [PubMed: 18988843]
2. Villella A, Hall JC. Neurogenetics of courtship and mating in Drosophila. Adv Genet. 2008; 62:67–184. [PubMed: 19010254]
3. Zarkower D. Invertebrates may not be so different after all. Novartis Found Symp. 2002; 244:115–126. discussion 126-135, 203-116, 253-117. [PubMed: 11990787]
4. Williams TM, et al. The regulation and evolution of a genetic switch controlling sexually dimorphic traits in Drosophila. Cell. 2008; 134:610–623. [PubMed: 18724934]
5. Ng CS, Kopp A. Sex combs are important for male mating success in Drosophila melanogaster. Behav Genet. 2008; 38:195–201. [PubMed: 18213513]
6. Bray S, Amrein H. A putative Drosophila pheromone receptor expressed in male-specific taste neurons is required for efficient courtship. Neuron. 2003; 39:1019–1029. [PubMed: 12971900]
7. Dauwalder B. Systems behavior: of male courtship, the nervous system and beyond in Drosophila. Curr Genomics. 2008; 9:517–524. [PubMed: 19516958]
8. Waterbury JA, Jackson LL, Schedl P. Analysis of the doublesex female protein in Drosophila melanogaster: role on sexual differentiation and behavior and dependence on intersex. Genetics. 1999; 152:1653–1667. [PubMed: 10430590]
9. Shirangi TR, Dufour HD, Williams TM, Carroll SB. Rapid evolution of sex pheromone-producing enzyme expression in Drosophila. PLoS Biol. 2009; 7:e1000168. [PubMed: 19652700]
10. Manoli DS, et al. Male-specific fruitless specifies the neural substrates of Drosophila courtship behaviour. Nature. 2005; 436:395–400. [PubMed: 15959468]
11. Demir E, Dickson BJ. fruitless splicing specifies male courtship behavior in Drosophila. Cell. 2005; 121:785–794. [PubMed: 15935764]
12. Kimura K, Ote M, Tazawa T, Yamamoto D. Fruitless specifies sexually dimorphic neural circuitry in the Drosophila brain. Nature. 2005; 438:229–233. [PubMed: 16281036]
13. Lee G, et al. Spatial, temporal, and sexually dimorphic expression patterns of the fruitless gene in the Drosophila central nervous system. J Neurobiol. 2000; 43:404–426. [PubMed: 10861565]
14. Rideout EJ, Billeter JC, Goodwin SF. The sex-determination genes fruitless and doublesex specify a neural substrate required for courtship song. Curr Biol. 2007; 17:1473–1478. [PubMed: 17716899]
15. Villella A, Hall JC. Courtship anomalies caused by doublesex mutations in Drosophila melanogaster. Genetics. 1996; 143:331–344. [PubMed: 8722785]
16. Lee G, Hall JC, Park JH. Doublesex gene expression in the central nervous system of Drosophila melanogaster. J Neurogenet. 2002; 16:229–248. [PubMed: 12745633]
17. Sanders LE, Arbeitman MN. Doublesex establishes sexual dimorphism in the Drosophila central nervous system in an isoform-dependent manner by directing cell number. Dev Biol. 2008; 320:378–390. [PubMed: 18599032]
18. Billeter JC, et al. Isoform-specific control of male neuronal differentiation and behavior in Drosophila by the fruitless gene. Curr Biol. 2006; 16:1063–1076. [PubMed: 16753560]
19. Shirangi TR, Taylor BJ, McKeown M. A double-switch system regulates male courtship behavior in male and female Drosophila melanogaster. Nat Genet. 2006; 38:1435–1439. [PubMed: 17086183]
20. Kimura K, Hachiya T, Koganezawa M, Tazawa T, Yamamoto D. Fruitless and doublesex coordinate to generate male-specific neurons that can initiate courtship. Neuron. 2008; 59:759–769. [PubMed: 18786359]
21. Siwicki KK, Kravitz EA. Fruitless, doublesex and the genetics of social behavior in Drosophila melanogaster. Curr Opin Neurobiol. 2009; 19:200–206. [PubMed: 19541474]
22. Camara N, Whitworth C, Van Doren M. The creation of sexual dimorphism in the Drosophila soma. Curr Top Dev Biol. 2008; 83:65–107. [PubMed: 19118664]
23. Baker BS, Ridge KA. Sex and the single cell. I. On the action of major loci affecting sex determination in Drosophila melanogaster. Genetics. 1980; 94:383–423. [PubMed: 6771185]

Europe PMC Funders Author Manuscripts

24. Belote JM, Baker BS. Sexual behavior: its genetic control during development and adulthood in Drosophila melanogaster. Proc Natl Acad Sci U S A. 1987; 84:8026–8030. [PubMed: 3120181]
25. Bernstein AS, Neumann EK, Hall JC. Temporal analysis of tone pulses within the courtship songs of two sibling *Drosophila* species, their interspecific hybrid, and behavioral mutants of *D.melanogaster*. J Insect Behav. 1992; 5:15–36.
26. Kopp A, Duncan I, Godt D, Carroll SB. Genetic control and evolution of sexually dimorphic characters in Drosophila. Nature. 2000; 408:553–559. [PubMed: 11117736]
27. Montell C. A taste of the Drosophila gustatory receptors. Curr Opin Neurobiol. 2009; 19:345–353. [PubMed: 19660932]
28. von Schilcher F, Hall JC. Neural topography of courtship song in sex mosaics of Drosophila melanogaster. J Comp Physiol A. 1979; 129:85–95.
29. Clyne JD, Miesenbock G. Sex-specific control and tuning of the pattern generator for courtship song in Drosophila. Cell. 2008; 133:354–363. [PubMed: 18423205]
30. Possidente DR, Murphey RK. Genetic control of sexually dimorphic axon morphology in Drosophila sensory neurons. Dev Biol. 1989; 132:448–457. [PubMed: 2924997]
31. MacDonald JM, et al. The Drosophila cell corpse engulfment receptor Draper mediates glial clearance of severed axons. Neuron. 2006; 50:869–881. [PubMed: 16772169]
32. Hay BA, Wolff T, Rubin GM. Expression of baculovirus P35 prevents cell death in Drosophila. Development. 1994; 120:2121–2129. [PubMed: 7925015]
33. Sweeney ST, Broadie K, Keane J, Niemann H, O'Kane CJ. Targeted expression of tetanus toxin light chain in Drosophila specifically eliminates synaptic transmission and causes behavioral defects. Neuron. 1995; 14:341–351. [PubMed: 7857643]
34. Santel A, Winhauer T, Blumer N, Renkawitz-Pohl R. The Drosophila don juan (dj) gene encodes a novel sperm specific protein component characterized by an unusual domain of a repetitive amino acid motif. Mech Dev. 1997; 64:19–30. [PubMed: 9232593]
35. Villella A, Peyre JB, Aigaki T, Hall JC. Defective transfer of seminal-fluid materials during matings of semi-fertile fruitless mutants in Drosophila. J Comp Physiol A Neuroethol Sens Neural Behav Physiol. 2006; 192:1253–1269. [PubMed: 16896687]
36. Billeter JC, Rideout EJ, Dornan AJ, Goodwin SF. Control of male sexual behavior in Drosophila by the sex determination pathway. Curr Biol. 2006; 16:R766–776. [PubMed: 16950103]
37. Hall JC. Portions of the central nervous system controlling reproductive behavior in Drosophila melanogaster. Behav Genet. 1977; 7:291–312. [PubMed: 410405]
38. Hall JC. Control of male reproductive behavior by the central nervous system of Drosophila: dissection of a courtship pathway by genetic mosaics. Genetics. 1979; 92:437–457. [PubMed: 114447]
39. Ferveur JF, Greenspan RJ. Courtship behavior of brain mosaics in Drosophila. J Neurogenet. 1998; 12:205–226. [PubMed: 10656109]
40. Manoli DS, Baker BS. Median bundle neurons coordinate behaviours during Drosophila male courtship. Nature. 2004; 430:564–569. [PubMed: 15282607]
41. Broughton SJ, Kitamoto T, Greenspan RJ. Excitatory and inhibitory switches for courtship in the brain of Drosophila melanogaster. Curr Biol. 2004; 14:538–547. [PubMed: 15062094]
42. Hasemeyer M, Yapici N, Heberlein U, Dickson BJ. Sensory neurons in the Drosophila genital tract regulate female reproductive behavior. Neuron. 2009; 61:511–518. [PubMed: 19249272]
43. Yang CH, et al. Control of the postmating behavioral switch in Drosophila females by internal sensory neurons. Neuron. 2009; 61:519–526. [PubMed: 19249273]
44. Lazareva AA, Roman G, Mattox W, Hardin PE, Dauwalder B. A role for the adult fat body in Drosophila male courtship behavior. PLoS Genet. 2007; 3:e16. [PubMed: 17257054]
45. Rong YS, Golic KG. Gene targeting by homologous recombination in Drosophila. Science. 2000; 288:2013–2018. [PubMed: 10856208]
46. Billeter JC, Goodwin SF. Characterization of Drosophila fruitless-gal4 transgenes reveals expression in male-specific fruitless neurons and innervation of male reproductive structures. J Comp Neurol. 2004; 475:270–287. [PubMed: 15211467]

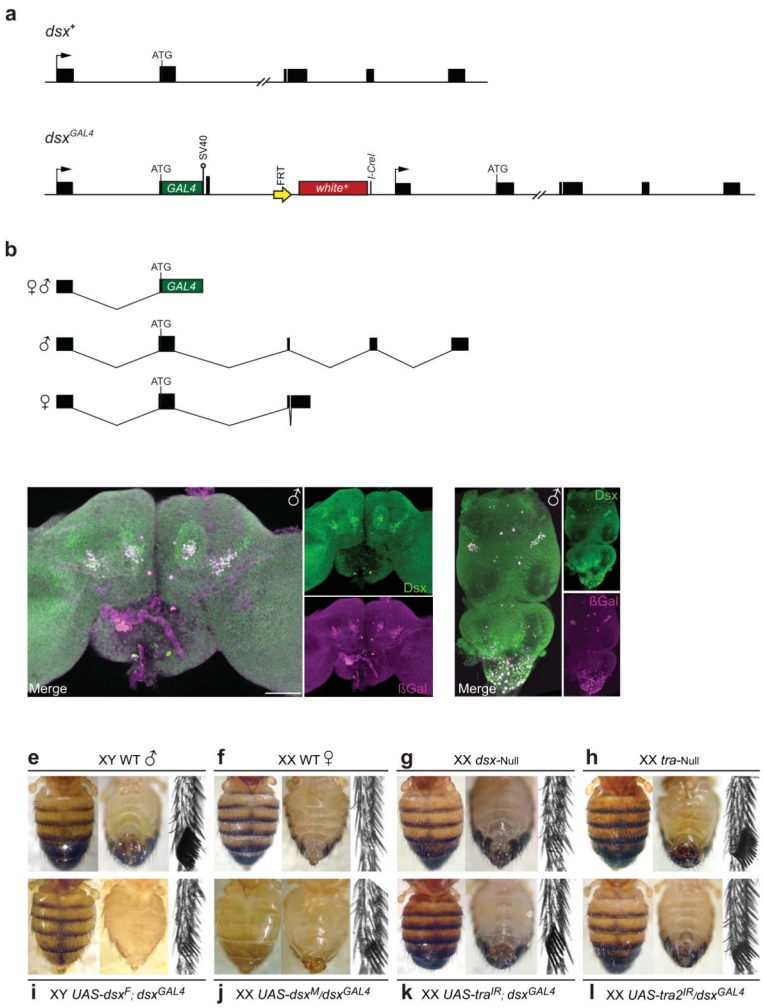

Figure 1.

Expression of GAL4 from the *dsx* locus recapitulates endogenous *dsx* expression. (**a**) Schematic of *dsx* (*dsx*$^{+}$) and *GAL4* knock-in allele (*dsx*^{GAL4}). Transcriptional start sites, arrows; black boxes, exons. (**b**) Male and female *dsx*^{GAL4} locus predicted transcripts. (**c,d**) *dsx*^{GAL4}, *UAS-nlacZ* 2-day-old male pupa. anti-Dsx (green), anti-ßGal (magenta). (**c**) Brain and (**d**) VNC. Ventral views; anterior up. Scale bars = 50 μm. (**e-l**) *dsx*^{GAL4} transformation of secondary sexual characteristics; dorsal abdominal cuticular pigmentation; external genitalia; T1 leg basitarsal detail. (**e**) XY and (**f**) XX wild-type. (**g**) XX *dsx*-null intersexual. (**h**) XX *tra*-null pseudo-male. (**i**) XY *UAS-dsx*^{F};*dsx*^{GAL4} pseudo-female. (**j**) XX *dsx*^{GAL4}/*UAS-dsx*^{M} pseudo-male. (**k**) XX *UAS-tra*^{IR};*dsx*^{GAL4}. (**l**) XX *dsx*^{GAL4}/*UAS-tra2*^{IR}.

Europe PMC Funders Author Manuscripts

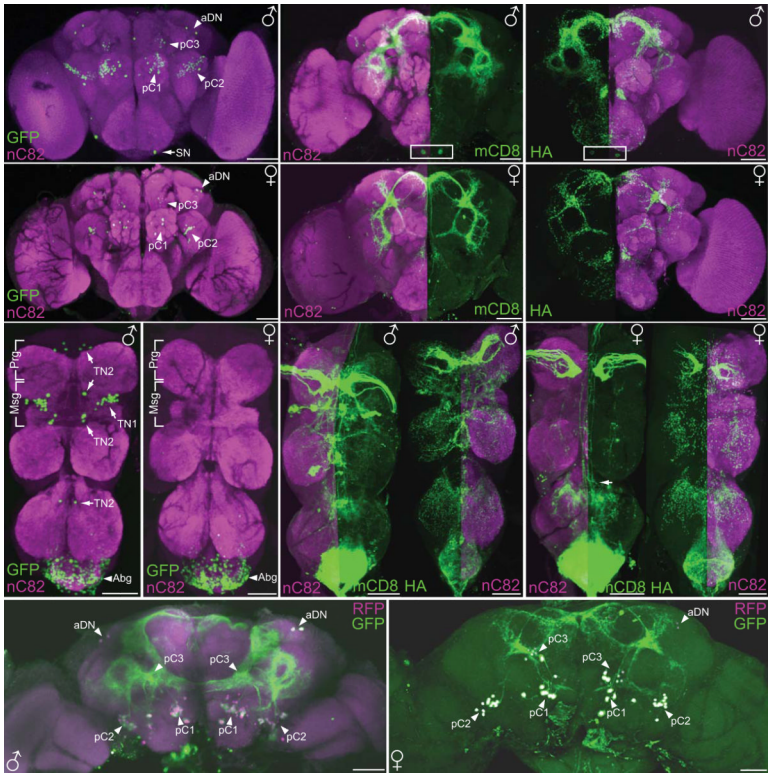

Figure 2.

Sexually dimorphic expression of *dsx*^{GAL4}-neurons and associated projections and colocalization with Fru^{M} in 3-5 day adult CNSs. (**a**) Male brain, *dsx* neuronal clusters (arrowheads), male-specific SN neurons (only one cell in plane of focus; arrow). The cell bodies of pC1 ,pC2, and pC3 in dorsal inferomedial, inferolateral, and superomedial protocerebral areas respectively. (**b,c**) Male brain, SN cells position, boxed. (**d-f**) Female brain; (**d**) *dsx* neuronal clusters (arrowheads). (**g**) Male VNC, Abg cluster (arrowhead), male-specific TN1 and TN2 neurons (arrow). (**h**) Female VNC, Abg cluster (arrowhead). (**i,j**) Male VNC. (**k**) Female VNC, hindleg contralateral projection (arrow). (**l**) Female VNC. (**a,d,g,h**) Neuronal cell bodies expressing *UAS-pStingerII* (nGFP). anti-GFP (green). (**b,e,i,k**) Neuronal projections expressing *UAS-mCD8::GFP* (membrane-bound GFP), anti-mCD8 (green). (**c,f,j,l**) Synaptic expression; expressing *UAS-synaptotagmin* (pre-synaptic marker) tagged with HA, anti-HA (green). Neuropil counterstained with anti-nC82 (magenta). Ventral views; anterior top. (**m**) *UAS-RedStinger*;*dsx*^{GAL4}, *UAS-mCD8::GFP* male and (**n**) female brain. Dsx neuronal clusters (arrowheads). anti-RFP(magenta); anti-GFP (green). Horizontal view, ventral top. Scale bars = 50 μm.

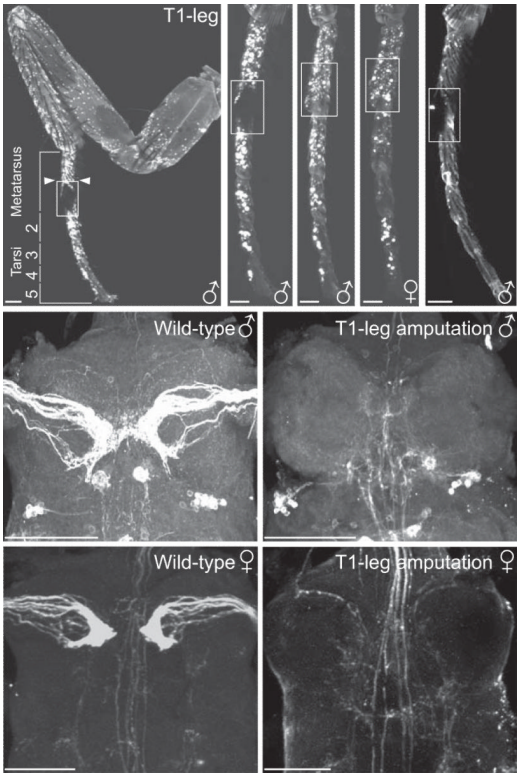

Figure 3.

Sex apecific *dsx*^{GAL4} expression in the foreleg and effect of basitarsal amputations on axonal projections. (**a-d**) Sexually dimorphic expression in T1 foreleg. (**a**) Male T1 leg (medial aspect), sex comb (boxed). *dsx*^{GAL4} expressing cells in metatarsus = 96 ± 14.4 (n=7) and tarsi 2-5 = 72 ± 10.0 (n=7) (**b**) Medial and (**c**) lateral aspect male T1 tarsi and metatarsus, sex comb (boxed). (**d**) Female T1 tarsi and metatarsus (lateral aspect), area consistent with sex comb (boxed). *dsx*^{GAL4} expressing cells in metatarsus = 77 ± 12.4 (n=8) and tarsi 2-5 = 58 ± 9.7 (n=7) (**e**) Male T1 tarsi and metatarsus (medial aspect), *elav-GAL80* repression in subset of *dsx*^{GAL4} cells, metatarsal sex comb (boxed). (**f**) Wild-type male and (**h**) wild-type female prothoracic axonal projections (close-up from Fig. 2k). (**g**) Atrophied male and (**i**) atrophied female prothoracic axonal projections, post-amputation. Point of amputation, arrowheads (**a**). Scale bar = 50 μm.

Europe PMC Funders Author Manuscripts

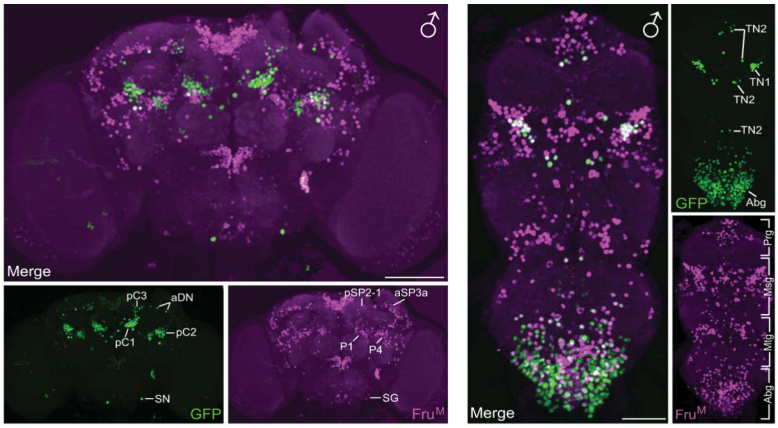

Figure 4.

Co-localization of Fru^{M} neuronal cells and *dsx*^{GAL4} cells (expressing UAS-nGFP) in 3-day-old adult male. anti-nGFP (green), anti-Fru^{M} (magenta). (**a**) Brain; Dorsal view; anterior up. *dsx* and Fru^{M} neuronal cells and clusters designated. (**b**) VNC. Ventral view; anterior up. *dsx* and Fru^{M} neuronal cells and clusters that colocalize, designated. Fru^{M} clusters as previously described20. Scale bars = 50 μm.

Europe PMC Funders Author Manuscripts

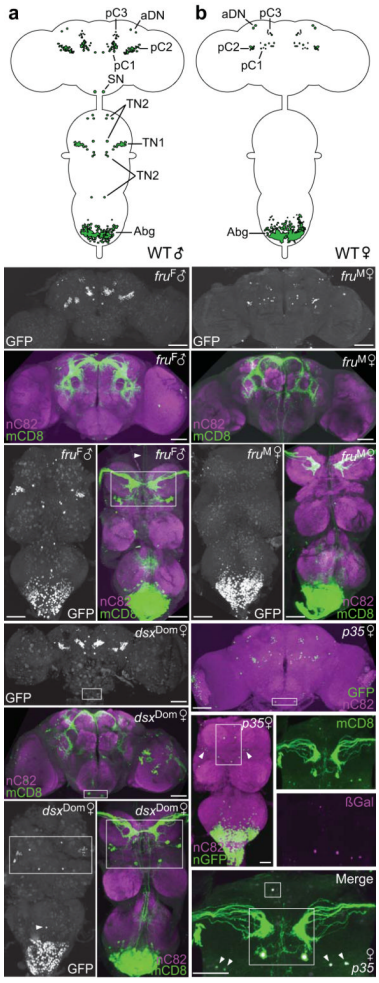

Figure 5.

dsx^{GAL4} expression in CNSs of Fru^{M}-null males and females expressing Fru^{M} or the anti-apoptotic transgene *UAS-p35*. (**a,b**) Schematic of *dsx*^{GAL4} nGFP expression in wild-type adult male (**a**) and female (**b**) CNSs. Individual neuronal clusters designated. (**c**) nGFP and (**d**) Membrane-bound GFP in Fru^{M}-null adult male brain. (**e**) nGFP and (**f**) Membrane-bound GFP in Fru^{M}-null adult male VNC, reduction in prothoracic contralateral (boxed area) and cervical connection projections (arrowhead). (**g**) nGFP and (**h**) membrane-bound GFP in adult female brain expressing Fru^{M}. (**i**) nGFP and (**j** membrane-bound GFP in adult female VNC expressing Fru^{M}. (**k**) nGFP and (**l**) membrane-bound GFP in adult female brain expressing both Dsx^{F} and Dsx^{M}. Supernumerary SN cells (boxed area). (**m**) nGFP adult female VNC expressing both Dsx^{F} and Dsx^{M}. Supernumerary male-specific TN1 and TN2 cells (boxed area, arrow). (**n**) Membrane-bound GFP in adult female brain expressing both Dsx^{F} and Dsx^{M}. Prothoracic contralateral projections (boxed area). (**o**) *UAS-p35*;*dsx*^{GAL4} adult female brain, supernumerary SN cells (boxed area). (**p**) *UAS-p35*;*dsx*^{GAL4} adult female VNC, supernumerary TN1 (arrowheads) and TN2 (boxed area) neurons. (**q-s**) *UAS-nLacZ,-mCD8::GFP,-p35*;*dsx*^{GAL4} adult female prothoracic ganglion (Prg) (**q**) Merged image, co-expression of membrane-bound GFP, green (**r**) and nuclear ßGal, magenta (**s**). Supernumerary TN1 (arrowheads) and TN2 cells (boxed area) and ectopic contralateral projections. Ventral views; anterior up. (**c**, **e**, **g**, **i**, **k**, **m**) anti-GFP, green. (**d**, **f**, **h**, **j**, **l**, **n**, **o**, **p**) anti-mCD8, green and neuropil counter-stained with anti-nC82, magenta. Genotypes as per Methods. Scale bar = 50 μm

Europe PMC Funders Author Manuscripts

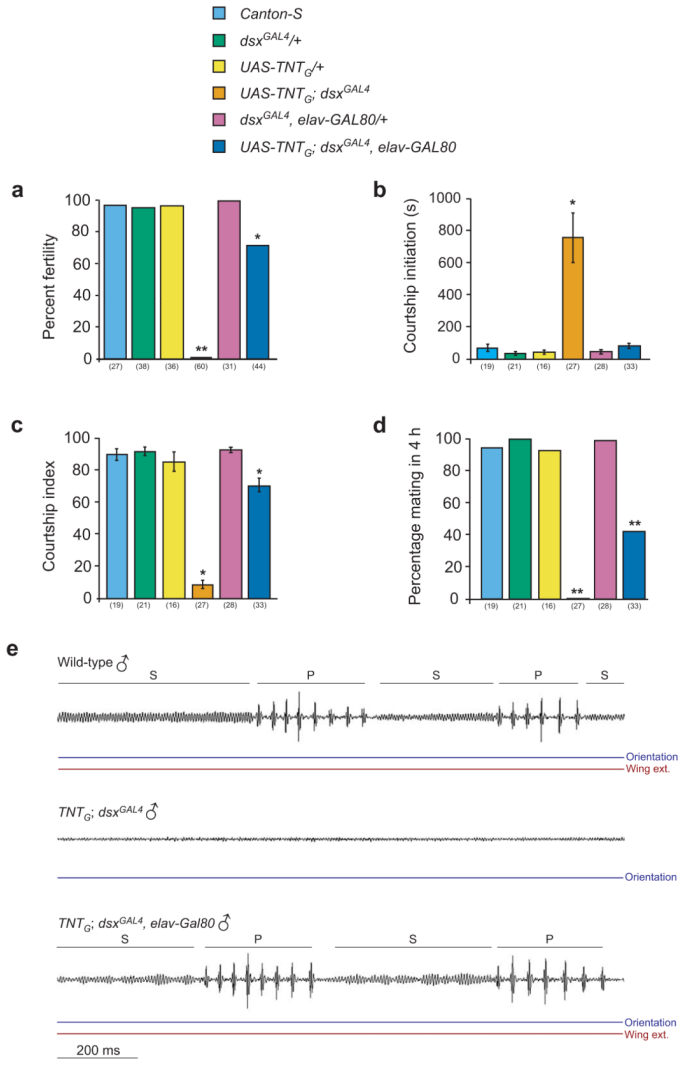

Figure 6.

dsx^{GAL4} neurons control male sexual behavior. (**a**) Male fertility. p-values * <0.05, ** <0.0001 (Fisher Exact Test). (**b**) Courtship initiation. Mean ± SEM. p-values * <0.05 (Tukey-Kramer HSD statistical test). (**c**) Courtship index. Mean ± SEM. p-values * <0.05 (Tukey-Kramer HSD test). (**d**) Percentage males mating in 4-h. p-values ** <0.0001 (Fisher Exact Test). (**e**) Song-recording, 5-7 day old males. Pulse (P) and sine (S) song components indicated above traces, courtship display below. Each trace represents a fraction of a 10 min recording. Scale bar= 200 ms. Genotypes indicate males. Target females, wild-type. Wild-type males, (15); 18.6 ± 2.2 sine bouts per min (SBPM), 19.9 ± 1.4 pulse trains per min (PTPM), 8.1 ± 0.3 mean pulses per train (MPPT), 31.7 ± 3.0 interpulse interval (IPI, ms). *UAS-TNT*$_G$; *dsx*^{GAL4} males, (10); no recordable data. *UAS-TNT*$_G$; *dsx*^{GAL4}, *elav-GAL80* males, (10); 18.4 ± 1.5 (SBPM), 26.6 ± 3.8 (PTPM), 10.0 ± 0.4 (MPPT), 34.0 ± 0.4 (IPI, ms). Mean ± SEM. n's in parentheses.

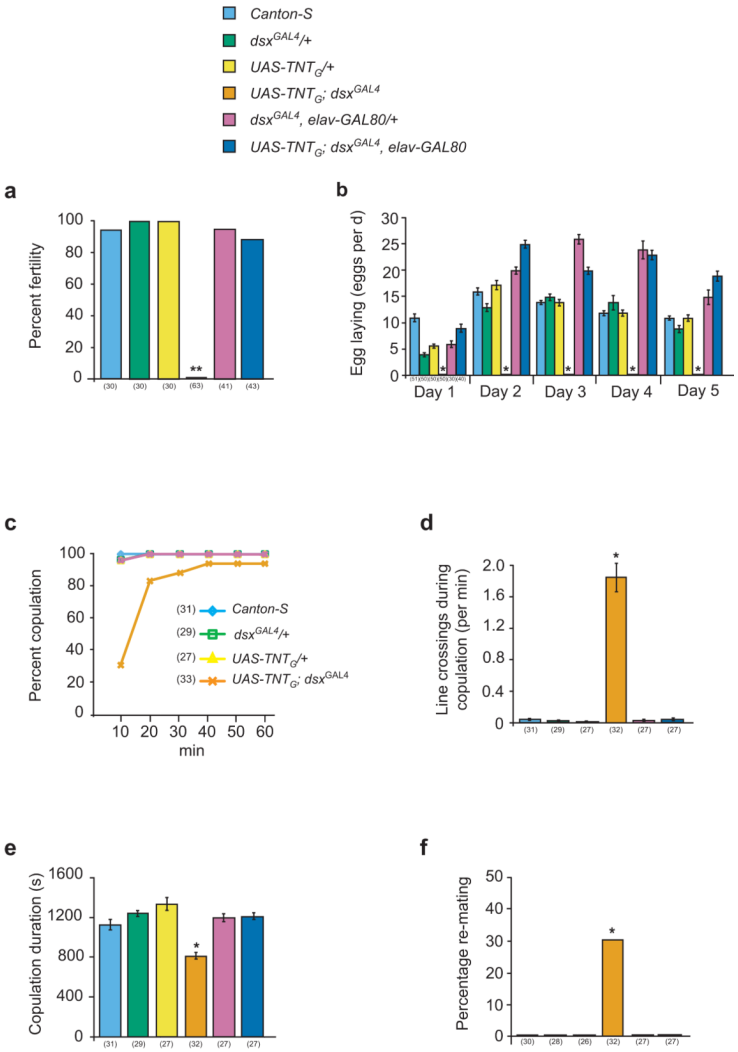

Figure 7.

dsx^{GAL4} neurons control female sexual behavior. (**a**) Female fertility. p-values ** <0.0001 (Fisher Exact Test). (**b**) Egg-laying. Mean ± SEM. p-values * <0.0001 (Dunnett's Test). (**c**) Percent copulation over time (10 minute intervals for 1 h). (**d**) Line crossings during copulation. Mean ± SEM. p-values * <0.05 (Tukey-Kramer HSD test). (**e**) Copulation duration. Mean ± SEM. p-values * <0.05 (Tukey-Kramer HSD test). (**f**) Percentage females re-mating with the same male in 4 h. p-values * <0.05 (Tukey-Kramer HSD test). Genotypes indicate females. Target males, wild-type. n's in parentheses.

Europe PMC Funders Author Manuscripts

Europe PMC Funders Author Manuscripts

Nat Neurosci. Author manuscript; available in PMC 2011 May 11.

Table 1

dsx^{GAL4} driven nGFP expression in CNSs of Fru^M-null males and females expressing Fru^M, Dsx^M, or p35

	5-day-old Adult Male		5-day-old Adult Female			
	wild-type (*CS*)	***fru*^{F}/*dsx*^{GAL4}, *Df(3R)fru*$^{4-40}$**	**wild-type (*CS*)**	***fru*^{M}/*dsx*^{GAL4}, *Df(3R)fru*$^{4-40}$**	***dsx*^{GAL4}/*dsx*^{Dom}**	***UAS-p35*; *dsx*^{GAL4}**
Fru^M	+	−	−	+	−	−
Dsx^M	+	+	−	−	+	−
Dsx^F	−	−	+	+	+	+
Neuronal clusters						
Brain						
-PC1	56.9 ± 5.0	48.2 ± 8.6 **	8.7± 2.0	9.6 ± 1.1	45.8 ± 6.4 **	11.1 ± 2.8
-PC2	78.6 ± 3.1	67.4 ± 8.8 *	11.2 ± 1.9	10.7 ± 1.5	56.3 ± 4.7 **	16.1 ± 1.8 *
-PC3	13.6 ± 1.0	10.7 ± 1.2 **	6.4 ± 1.4	6.3 ± 1.9	7.0 ± 1.3	11.7± 2.1 **
-SN	1 ± 0	1 ± 0	0 ± 0	0 ± 0	1 ± 0 **	1.0 ± 0 **
-aDN	2 ± 0	2 ± 0	2 ± 0	2 ± 0	2 ± 0	2.2 ± 0.4
Ventral Nerve Cord						
-TN1	22.4 ± 1.7	23.0 ± 2.2	0 ± 0	0 ± 0	15.5 ± 2.2 **	3.0 ± 0.6 **
-TN2	6.9 ± 3.0	6.6 ± 0.7	0 ± 0	0 ± 0	6.0 ± 2.5 **	7.0± 2.0 **

The presence or absence of Fru^M, Dsx^M, and Dsx^F expression is noted below genotypes. Counts represent one cluster per hemisegment. Mean ± standard deviation. n=10 for all genotypes.

* p-values <0.005

** p-values <0.0001.